Biophysical Aspects of Auger Processes, AAPM Symposium Series No. 8 (1992) 227-248
Eds. RW Howell, VR Narra, KSR Sastry, DV Rao

HIGH AND LOW-LET CYTOCIDAL EFFECTS OF DNA-ASSOCIATED IODINE-125

KURT G. HOFER[1], NANETTE VAN LOON[2]
MARTIN H. SCHNEIDERMAN[3], and DAVID E. CHARLTON[4]

[1]Institute of Molecular Biophysics, Florida State University, Tallahassee, FL 32306
[2]Laboratory of Radiobiology, University of California, San Francisco, CA 94143
[3]Department of Radiology, University of Nebraska Medical Center, Omaha, NE 68198
[4]Department of Physics, Concordia University, Montreal, Quebec, Canada H3G 1M8

ABSTRACT

Chinese hamster ovary (CHO) cells synchronized by mitotic selection were plated and resynchronized with aphidicolin at the G_1/S boundary of the cell cycle. Thirty minutes after release from the aphidicolin block the cells were pulse-labeled for 10 min with ^{125}I-iododeoxyuridine and cell samples were harvested for freezing and ^{125}I-decay accumulation at time intervals ranging from 15 min to 8 h after termination of labeling. Control studies were carried out on X irradiated cells and on cells labeled continuously throughout the S phase or pulse-labeled during different stages of the S phase. Cell survival was evaluated by the standard colony forming assay.

The survival data demonstrated a striking shift from a low-LET to a high-LET mode of action for ^{125}I-induced cell killing with increasing time intervals between DNA pulse-labeling and decay accumulation. Cells harvested and frozen within 1 h after pulse-labeling exhibited a low-LET dose-survival response with a pronounced shoulder and a large D_0 of up to 0.9 Gy. With longer post-labeling chase periods, the shoulder and the D_0 decreased progressively and cells harvested 5 h after pulse-labeling or later yielded the high-LET dose-survival response that is usually encountered with DNA-associated ^{125}I (D_0: 0.13 Gy).

Two alternative interpretations for these findings can be envisioned. (1) If it is assumed that DNA is the sole target for radiation death, the results indicate that DNA maturation increases radiation damage to DNA or reduces damage repair. (2) If radiation death involves damage to higher-order genome structures and/or associated nuclear matrix elements, the findings would suggest that newly replicated DNA is not attached to these structures during the initial low-LET period, but ^{125}I starts to induce high-LET effects as labeled DNA segments become associated with the target structure(s). On balance, our data favor the second of these alternatives.

INTRODUCTION

Biological damage from the decay of internal Auger emitters such as ^{125}I, ^{67}Ga, ^{77}Br, or ^{75}Se has been the subject of numerous investigations for more than 20 years (1-7). Due to their unique decay pattern, these radionuclides provide information on the fundamental mechanisms of radiation action not easily duplicated by other modes of cellular irradiation. The most widely used Auger emitter, ^{125}I, decays by electron capture and emits a shower of up to 50 electrons with energies ranging from a few eV to several tens of keV (8). Thus, unlike external radiation sources which usually irradiate the entire cell volume, Auger emitters decaying in any particular cell compartment cause highly differential radiation exposure to the labeled site, with only minor irradiation of distant subcellular regions (5,8,9).

It is believed that radiation-induced cell death in mammalian cells results primarily from damage to a target (or targets) located within the cell nucleus (10,11). Support for this notion is derived from studies where Auger emitters are incorporated into different cell compartments such as the plasma membrane (12), lysosomes (5), mitochondria (13), the general cytoplasm (6), or

nuclear DNA (1-5,7,9,12). The results prove that even massive radiation doses to the plasma membrane or cytoplasmic organelles are relatively nontoxic, but when ^{125}I is incorporated into nuclear DNA via the thymidine analogue ^{125}I-iododeoxyuridine ($^{125}IUdR$), the high local energy deposition within the genome results in extreme, high-LET like, radiation lethality.

In this report we present evidence that the radiobiological consequences of ^{125}I can be variable even if the radionuclide is incorporated into DNA. When cells are pulse-labeled with $^{125}IUdR$ and harvested for decay accumulation at different time intervals after labeling, ^{125}I-decays in the DNA can result in biological effects that resemble either low-LET or high-LET radiation damage. These unexpected findings suggest that ^{125}I toxicity may be related to changes in chromatin organization and/or variations in distance between decay events and potential critical targets within the cell at different times after DNA replication.

MATERIALS AND METHODS

Cell Synchronization

Chinese hamster ovary (CHO) cells were grown as monolayers on 25 cm^2 or 75 cm^2 Falcon plastic flasks, at 37°C, in a humidified atmosphere of 5% CO_2 in air. The growth medium was modified McCoy's 5a supplemented with 5% calf bovine serum, 100 units/ml penicillin-G and 100 μg/ml streptomycin. Under these conditions the population doubling time during exponential growth was 12-13 h (14) with a 3-4 h G_1 phase (15), 7 h S phase, 1.25 h G_2 phase (16), and 0.75 h M phase (17). To avoid genetic drift, new cultures were initiated from frozen stocks every 6 weeks. The stock cultures, carried without antibiotics, were used only if they tested free of mycoplasma using the Gibco Myco Tect test.

Prior to synchronization by mitotic cell selection, 4.5×10^6 CHO cells were plated into each of ten 75 cm^2 flasks. At the start of selection (about 18 h after plating) each flask contained $1.3\text{-}1.7 \times 10^7$ cells in exponential growth. Mitotic cells were selectively detached from this population during a 15 s selection shake as previously described (16,17). The mitotic cells were harvested and immediately cooled to 4°C. The cells remaining on the flask were refed with temperature and pH adjusted medium. The entire procedure (selection, harvesting, and refeeding) took less than 30 s and was carried out

aseptically in a portable selection apparatus specifically designed to maintain the temperature and pH of the medium. The apparatus basically consisted of a large, custom-made 37°C CO_2 incubator outfitted with a reciprocal shaker and a complex pumping system that permitted simultaneous semi-automatic cell harvest from up to 10 flasks by vacuum suction and subsequent refeeding of the flasks by a motor-driven multiple syringe system. The mitotic cell selection procedure was repeated every 10 min for up to 8 h. With repeated harvests, up to 5×10^7 mitotic cells with a mitotic index of 98% or higher were collected in a single experiment.

After harvesting, the mitotic cells were pooled, pelleted by centrifugation at 4°C, and resuspended in "cryoprotectant medium" (Ham's F10 supplemented with 15% bovine calf serum and 10% DMSO). Aliquots of the cell suspension (1 ml) were pipetted into 2 ml Nalgene Cryovials, and the tightly closed vials were placed into a rack and immersed in upright position into 100 ml of ethanol in a flat-bottom glass container with a screw-cap top. The container was then placed into a -90°C deep-freezer for 60 min. This procedure resulted in slow freezing of the cell suspension at a rate of 1.5-2.0°C/min as monitored on cell samples frozen in modified Cryovials outfitted with a low temperature thermometer (heavily insulated except for bulb region). After 60 min the vials were removed from the ethanol bath and transferred to liquid nitrogen storage for future use. The freezing and thawing procedure did not affect cell viability as determined by the standard colony forming assay and did not induce any detectable changes in cell cycle traverse after replating.

^{125}I Toxicity Studies

Carrier-free ^{125}IUdR (specific activity: 82.14 PBq/mol) was synthesized in this laboratory as described previously (18). Before use, the ^{125}IUdR was purified by HPLC on a Beckman Ultrasphere reverse phase column (5 µm spherical 80 A pore, 250 X 4.6 mm). The purification procedure involved an initial elution step (15 min at 1 ml/min) with a buffer containing 4.75 mM KH_2PO_4 dissolved in 1.5% ethanol/water and adjusted to pH 4.0 with concentrated H_3PO_4, followed by elution of ^{125}IUdR with a buffer containing 4mM KH_2PO_4 in 6% ethanol/water, adjusted to pH 4.0 with concentrated H_3PO_4. In this second elution step (also at 1 ml/min) the ^{125}IUdR peak eluted with fraction 17 or 18.

For ^{125}IUdR labeling, samples of frozen mitotic cells were thawed by immersion in a 37°C water bath. The cells were then pelleted by centrifugation, suspended in fresh temperature and pH adjusted McCoy's 5a, and plated in 25 cm^2 flasks. After 1 h incubation at 37°C, when the cells had completed mitosis and had become attached to the flask, aphidicolin (APC, 5 μg/ml) was added to the medium for 7 h to block the cells at the G_1/S boundary of the cell cycle (19). Exposure to APC did not affect the viability of the cells, but did shorten the subsequent S phase from the usual 7 h to about 5.5 h.

After removal of APC, cells were subjected to 10 min pulse-labeling with ^{125}IUdR (12-25 kBq/ml in McCoy's 5a with no added thymidine) during different stages of the S phase. For comparison, other groups of cells were labeled continually throughout the S phase (1.25 kBq/ml, with 1×10^{-6} M thymidine added to the medium). Labeling was terminated by discarding the labeling medium and rinsing the cells three times with 5 ml of temperature and pH adjusted medium. After refeeding, the cells were returned to the 37°C incubator. Depending on the requirements of the experiment, cells from individual flasks were harvested at time intervals ranging from 15 min to 8 h after termination of labeling. The number of cells harvested from each flask was evaluated by counting on a Coulter Model B particle counter.

The radionuclide content per cell was evaluated by precipitating known numbers of labeled cells (in some cases with approximately 10^6 "carrier" cells) with ice-cold 10% TCA. The ^{125}I content of the cell pellet was determined in a calibrated well-type crystal scintillation counter. Additional cell samples were retained for autoradiographic examination of the labeling index (98% or higher in all experimental groups). To permit accumulation of ^{125}I damage under controlled conditions, the remaining labeled cells were suspended in cryoprotectant medium and cell aliquots were frozen and stored in liquid nitrogen as described above.

At the time of freezing the cells sustained ^{125}I-decays at a rate of 0.4 to 0.8 decays/cell/h. Depending on the required number of decays/cell, the storage time in liquid nitrogen ranged from 1 h to 5 weeks. The 1 h group served as the "zero decay" control group, *i.e.*, the 1-6 ^{125}I-decays that had occurred in the cells up to this point were disregarded and accumulation of decays in all experimental groups was assumed to start 1 h after the onset of liquid nitrogen storage. This procedure produced a significant underestimate of the actual number of ^{125}I decays experienced by cells removed from storage

after short accumulation periods but did not significantly affect the dose calculations for cells stored in liquid nitrogen for prolonged periods of time.

After the frozen cells had accumulated the desired number of ^{125}I-decays, cell samples were removed from cold storage, thawed, and diluted in McCoy's 5a medium supplemented with 5% calf bovine serum and 10% fetal bovine serum. Three replicate plates (60 mm Petri dishes) were prepared for each experimental group. The dishes were incubated at 37°C for 7 days until the colonies were large enough for fixation and staining with 0.25% crystal violet. Unlabeled control cells subjected to all these procedures (including labeling with nonradioactive IUdR) exhibited a plating efficiency of between 70-80%.

X ray Studies

Cells synchronized by mitotic selection and subsequent treatment with APC (but not labeled with ^{125}IUdR) were harvested either during early-S phase (1 h after removal of APC) or in late-S/G_2 phase (6 h after removal of APC). The cells were suspended in cryoprotectant medium and irradiated with an X ray beam generated by a General Electric Maxitron 300 therapy machine operated at 250 kVp and 20 mA. The X ray beam was filtered with 1 mm copper (HVL 20 mm Al). The dose rate was 1 Gy/min as measured by a Victoreen ionization chamber. All irradiations were performed at 4°C and the cell samples were rotated at 18 rpm to ensure uniform dose distribution.

Microdosimetry Calculations

Microdosimetry calculations were performed for early-S phase cells (15 min chase group) and for late-S/G_2 cells (5 h chase group). The geometry and dimensions of the cell nuclei were evaluated by microscopic observation on a Nikon Microphot-FX microscope on cells fixed in 3:1 methanol:acetic acid. To account for possible shrinkage in the volume of the cell nucleus during freezing (20), the nuclear size measurements were performed on unfrozen and frozen cell samples. In the latter case, aliquots of the frozen cell suspensions were transferred directly from liquid nitrogen storage into 3:1 methanol:acetic acid and allowed to thaw in the presence of the fixative to preserve the nuclear morphology of frozen cells. It was found that in all cases tested the nuclear volume of frozen cells was about 30-35% lower than that of corresponding unfrozen control cells. For our dosimetry calculations the nuclei of frozen CHO cells were assumed to be ellipsoids with axial

dimensions of 4.95 μm X 3.55 μm X 3.55 μm (volume 261 μm^3) for cells in early-S phase and 6.95 μm X 4.68 μm X 4.68 μm (volume 637 μm^3) for cells in late-S/G_2.

Based on a method described by Charlton and Booz (8), the mean dose per decay to cell nuclei was calculated from a file of 1,000 individual ^{125}I electron spectra. The origins of the decays were chosen at random within the ellipsoids, and the electron tracks from each decay spectrum were examined using the electron track code MOCA7B of Paretzke (21). Each electron was followed to the end of its track or until the primary electron had left the ellipsoid and its distance from the nearest surface was sufficiently large to minimize the chance of back-scattering into the ellipsoid. From the sum of energy deposited inside the ellipsoid by all interactions (averaged over 914 decays for early-S phase nuclei and over 800 decays for late-S/G_2 phase nuclei), the average intranuclear energy deposition per ^{125}I-decay was calculated to be 11.2 keV (0.00687 Gy) for early-S phase nuclei and 11.8 keV (0.00296 Gy) for late-S/G_2 nuclei. The similarity in total energy deposition (11.2 versus 11.8 keV) was not unexpected because the dimensions of both early-S and late-S nuclei are sufficiently large to ensure that most Auger electrons deposit all of their energy within the nuclear volume.

To facilitate a comparison between DNA double-strand breaks (DSB) and cell survival, DSB/decay values were calculated for early-S phase cells (15 min chase group) and late-S/G_2 phase cells (5 h chase group). According to previous calculations (22,23), each ^{125}I-decay in the DNA produces approximately 0.8 DSB at the site of decay. A lesser number of additional breaks are produced by high-energy Auger electrons at sites distant from the decay event. Assuming a DNA content of 3.6×10^{12} daltons/cell at the beginning of the S phase (twice this amount at the end of the S), and using 1×10^{-11} DSB/Gy/dalton as an estimate for the yield of breaks from low-LET radiations, it can be calculated that 0.247 DSB/decay are produced in early-S phase cells and 0.213 DSB/decay in late-S/G_2 cells due to low-LET radiation exposure contributed by the high-energy Auger electrons. Thus, the total DSB yield/^{125}I-decay amounts to 1.047 DSB/decay for early-S phase cells and 1.013 DSB/decay for late-S/G_2 cells.

RESULTS

Figure 1 presents the results of an experiment where mitotic CHO cells were plated and resynchronized at the G_1/S boundary of the cell cycle with

APC. The cells were then allowed to progress through the S phase and subjected to 10 min pulse-labeling with ^{125}IUdR starting 0.5, 1.5, 2.5, 3.5, or 4.5 h after removal of APC. This labeling schedule resulted in selective incorporation of ^{125}IUdR into five different subfractions of the genome, *i.e.*, in each experimental group a different 10 min segment of DNA (about 2-5% of the entire DNA) was labeled, the remaining 95-98% of the DNA remained unlabeled. To achieve random labeling of the entire genome, groups of identically pretreated CHO cells were labeled with ^{125}IUdR throughout the S phase. After labeling, the cells were chased in ^{125}IUdR-free medium and harvested in the G_1/early-S phase of the next cell cycle for freezing and accumulation of ^{125}I-decays. As shown in Fig. 1, the dose-survival curves for all six labeling groups were identical. This indicates that DNA-associated ^{125}I produces equal cytocidal effects regardless of whether the decays are randomly distributed over the entire DNA or are restricted to different 2-5% subfractions of the genome.

Figure 2 shows survival values for CHO cells pulse-labeled with ^{125}IUdR for 10 min starting 0.5 h after release from APC. The cells were then chased in nonradioactive medium and cell aliquots were harvested for freezing and decay accumulation after chase periods ranging from 15 min to 8 h. In other words, THE SAME 10 MIN SEGMENT OF DNA WAS LABELED IN ALL EXPERIMENTAL GROUPS, ONLY THE DURATION OF THE POST-LABELING CHASE WAS VARIED. Nevertheless, there was a striking change in the survival response of different groups. Cells harvested for decay accumulation within 1 h of labeling showed greatly enhanced resistance to ^{125}I-decays, yielding low-LET dose-survival curves with a pronounced shoulder and a large D_0 of about 135 decays/cell. With longer post-labeling chase periods the shoulder and the D_0 progressively declined and cells harvested 5 h after labeling or later were as sensitive to ^{125}I damage as cells labeled uniformly throughout the S phase (D_0: 42 decays/cell). The chase experiment shown in Fig. 2 was repeated five times, including twice on cells that had not been resynchronized with APC at the G_1/S boundary, always with similar results.

It should be noted that during the post-labeling chase the cells continued to progress through the cell cycle. To determine whether the shift from low-LET to high-LET action shown in Fig. 2 might be related to cell cycle position at the time of harvest, the chase experiment was repeated on cells pulse-labeled in late-S phase, 4.5 h after release from APC. The results were

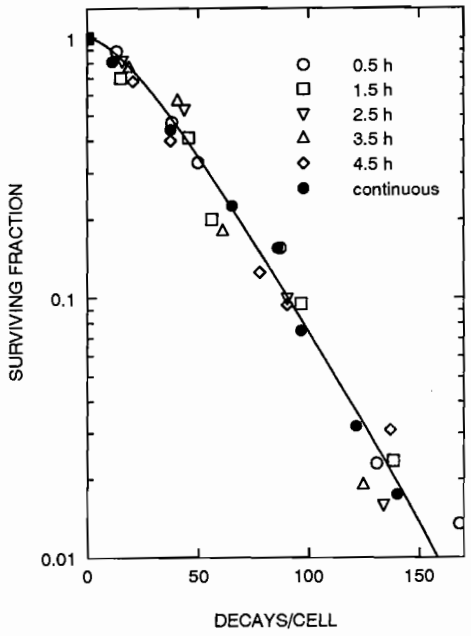

FIG. 1. Fractional survival of CHO cells ^{125}IUdR-labeled for 10 min at different times during the S phase (0.5, 1.5, 2.5, 3.5, 4.5 h after release from APC), and frozen for decay accumulation in the G_1/early-S phase of the next cell cycle. To compensate for increased ^{125}IUdR uptake during mid and late-S phase, the labeling dose was 28 kBq/ml, 22 kBq/ml, 14 kBq/ml, 12 kBq/ml, and 10 kBq/ml for the 0.5, 1.5, 2.5, 3.5 and 4.5 h groups, respectively. At the time of cell harvest in the G_1/early-S phase (after completion of one cell division), the exposure rate was 0.6-0.9 decays/cell/h. Using ^{125}I uptake ratios (pulse-labeled cells/continuously labeled cells) as a measure of fractional DNA replication during the 10 min labeling pulse indicates that about 1.8%, 2.3%, 4.2%, 4.7%, and 5.4% of the entire DNA was labeled in the 0.5, 1.5, 2.5, 3.5, and 4.5 h labeling groups, respectively.

similar to those shown in Fig. 2, that is, cells harvested for freezing and dose accumulation shortly after pulse-labeling exhibited a low-LET pattern of radiation death and cells harvested after prolonged post-labeling chase periods demonstrated a high-LET pattern of ^{125}I-induced radiation death (data

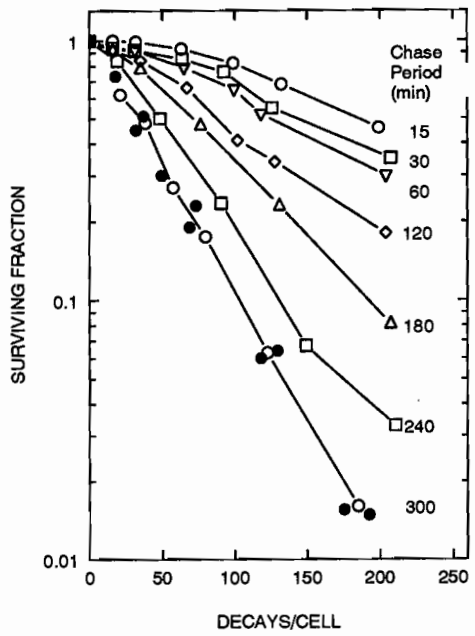

FIG. 2. Fractional survival of CHO cells pulse-labeled with ^{125}IUdR for 10 min starting 0.5 h after release from APC. The labeled cells were harvested for freezing and decay accumulation after post-labeling chase periods ranging from 15-480 min, but only values for up to 300 min are shown (open symbols). For comparison, survival values for cells labeled continuously through the S phase and harvested 3 h after termination of labeling are included (solid circles).

not shown). Expressed in terms of cell cycle position at the time of harvest, in experiments where cells were labeled 0.5 h after release from APC (Fig. 2), the 15 min chase group was located in early-S phase and the 5 h chase group in late-S/G_2 phase. In the second set of experiments, where cells were labeled 4.5 h after release from APC, the 15 min chase group was located in late-S phase and the 5 h chase group in the G_1 phase of the next cell cycle. Yet in both cases, regardless of cell cycle position, the 15 min chase group exhibited a low-LET pattern of ^{125}I-induced cell death and the 5 h chase group experienced high-LET type radiation lethality.

In another control experiment, mitotic CHO cells were plated and blocked at the G_1/S boundary with APC as described above and then X irradiated 1 h or 6 h after removal of APC. These two time points were chosen for X irradiation because they corresponded to the cell cycle positions occupied by the 15 min and 5 h ^{125}I chase groups at the time of harvesting and freezing. The results shown in Fig. 3 indicate a small difference in the X ray response of early-S phase cells (narrow shoulder, D_0 of 1.4 Gy) and late-S/G_2 cells (more pronounced shoulder, D_0 of 1.6 Gy), but this difference could not be responsible for the enhanced ^{125}I resistance of early-S phase cells shown in Fig. 2 because early-S phase cells exhibit enhanced (rather than reduced) sensitivity to X irradiation.

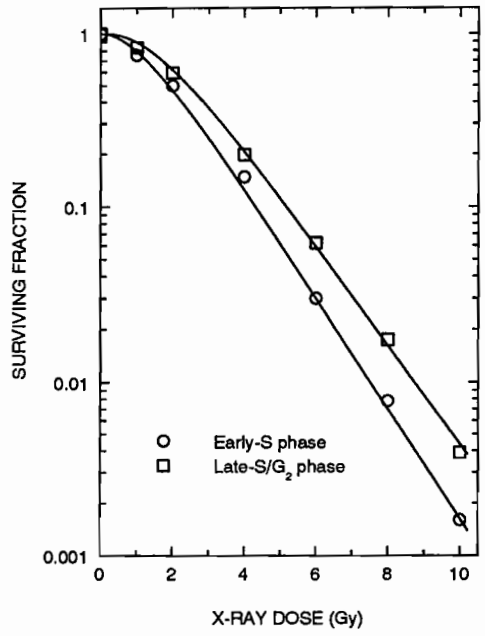

FIG. 3. Dose-survival curves for CHO cells subjected to X irradiation 1 h or 6 h after removal of APC.

To provide a more meaningful comparison between X ray and ^{125}I survival data, the ^{125}I-decay/cell values from Fig. 2 were converted to absorbed dose in Gy. Figure 4 shows the survival curves for the 15 min and

5 h chase groups as a function of dose to the cell nucleus. Using this method of presentation reveals that the ^{125}I response of the 15 min chase group is similar to that of the corresponding 1 h X ray group. In contrast, the ^{125}I survival curve for the 5 h chase shows a high-LET pattern with a D_0 of only 0.13 Gy, which is 12 times smaller than the D_0 of the corresponding 6 h X ray group. This comparison confirms the notion that depending on the time interval between $^{125}IUdR$ incorporation and decay accumulation, DNA-associated ^{125}I can produce either low-LET or high-LET radiation effects.

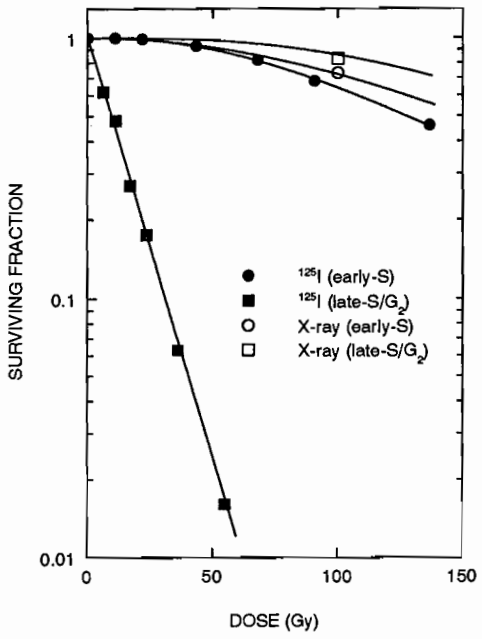

FIG. 4. ^{125}I dose-survival curves for CHO cells (15 min and 300 min chase groups from Fig. 2), plotted as a function of radiation dose to the cell nucleus (solid symbols). The values for CHO cells subjected to X irradiation at equivalent points in the cell cycle are indicated by the open symbols.

It is widely believed that a causative (or at least quantitative) link exists between DNA double-strand breaks (DSB) and radiation death (24,25). To test this hypothesis, the number of DNA DSB per ^{125}I-decay was calculated (22) for

early-S phase cells (15 min chase group) and late-S/G_2 phase cells (5 h chase group). According to these calculations about 1 DNA DSB/decay should be produced in both groups. This value agrees well with literature values for both naked oligonucleotide chains (26) and DNA in intact mammalian cells exposed to ^{125}I-decays under frozen conditions (27-29). Figure 5 shows the ^{125}I and X ray survival data from Figs. 2 and 3 plotted as a function of calculated DNA DSB/cell rather than absorbed dose in Gy. From this comparison it is clear that no obvious correlation between DNA DSB and cell lethality can be inferred from our data.

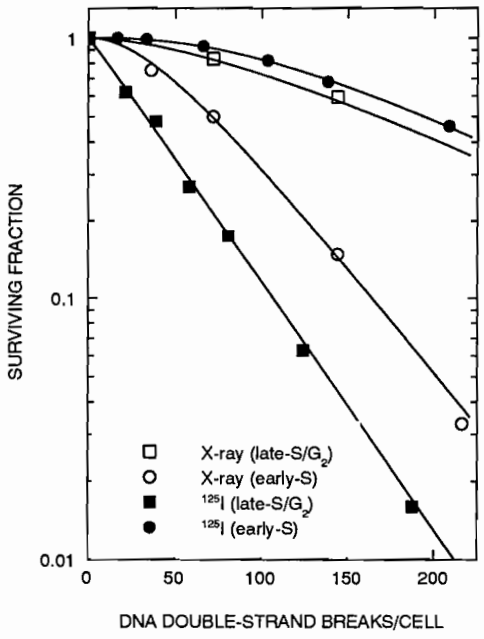

FIG. 5. ^{125}I dose-survival curves for CHO cells (15 min and 300 min chase groups from Fig. 2), plotted as a function of calculated DNA double-strand breaks/cell (solid symbols). The values for cells X irradiated at equivalent points in the cell cycle are indicated by the open symbols.

DISCUSSION

^{125}I Toxicity Studies

Previous radionuclide suicide studies on mammalian cells indicate that ^{125}I-decays in the DNA produce high-LET type radiation damage, but identical decay events at the plasma membrane, the cytoplasm, or specific cytoplasmic structures such as lysosomes or mitochondria yield low-LET dose survival curves with a shoulder and a large D_0 (1-9). Microdosimetric calculations suggest that these differences in biological action can be attributed to the unique decay and dose distribution characteristics of ^{125}I. The emission of a dense shower of low-energy Auger electrons results in highly localized deposition of radiation energy at the site of decay, with distant sites receiving only minor radiation doses from the few high-energy electrons emitted during ^{125}I-decay (5,8,9). Expressed differently, ^{125}I induces high-LET damage when the decay event takes place directly at the primary target site responsible for radiation death, but decays at sites distant from the primary target produce low-LET radiation effects. Although low-LET effects have been reported only for Auger emitters located outside the cell nucleus, similar low-LET cell killing can be expected for intranuclear decays if the decay site is sufficiently distant from the primary target to place the target outside the high-LET region around the site of ^{125}I decay.

The results reported here indicate that ^{125}I-decays at the DNA do not always result in high-LET radiation damage. Synchronized CHO cells pulse-labeled with ^{125}IUdR and frozen for decay accumulation within 1 h after labeling yield a low-LET survival response (Figs. 2 and 4) even though the ^{125}I-decays occur in close association with DNA. However, when cell harvesting and freezing are delayed for several hours, the cells exhibit the typical high-LET pattern of ^{125}I-induced radiation death. This marked shift in radiation action cannot be attributed to drug effects from cell synchronization because similar changes in the survival response can be observed on pulse-labeled cells that had not been resynchronized at the G_1/S boundary with aphidicolin. The shift is also not related to cell cycle progression during the chase period because the effect is observable regardless of whether cells are pulse-labeled in early-S phase or in late-S phase. It appears, therefore, that the low-LET to high-LET shift in the ^{125}I response represents a true shift in the cellular mechanism of ^{125}I-induced radiation death.

DNA Double-Strand Breaks and Cell Lethality

Several different hypotheses can be advanced to explain the findings described above. If it is assumed that DNA is the primary (or sole) target responsible for radiation death, the results indicate that DNA maturation increases the radiosensitivity of DNA, either by changing the type or amount of damage induced, or by decreasing damage repair. If radiation death involves damage to higher-order structures within the cell nucleus (*e.g.*, solenoid, DNA loop domain, nuclear matrix, nuclear envelope), the findings would suggest that ^{125}I is able to induce high-LET effects only after the labeled DNA segments have become part of (or attached to) the higher order target.

The first of these alternatives, enhanced radiation damage to mature DNA, appears to be the least likely explanation. There is no evidence that mature DNA is more radiosensitive than newly replicated DNA; it may in fact be more resistant to damage from low-LET radiations (30). However, even without invoking the prospect that mature DNA might show similarly enhanced resistance to ^{125}I effects, our results do not suggest any direct correlation between DNA DSB and cell lethality. ^{125}I administered in the form of ^{125}IUdR is covalently bound to DNA. Thus, regardless of the length of the post-labeling chase period, each ^{125}I-decay would be expected to produce DNA DSB with high efficiency (22,23,26-29), and the dose-survival curves for early and late harvested cells should become superimposed when fractional survival is plotted as a function of DSB/cell. No such correlation is apparent from the data shown in Fig. 5, *i.e.*, our findings argue against the widely held view that DNA DSB are directly linked to radiation death.

It might be postulated that even if the induction of DNA DSB is not linked to cell death, DNA repair may be more efficient in newly replicated DNA, resulting in enhanced cell survival after short post-labeling chase periods. However, preliminary repair studies using the neutral filter elution assay and gel electrophoresis do not support this interpretation (unpublished data). The repair hypothesis also conflicts with the finding that for the 15 min chase group (where ^{125}I-decays occur in newly replicated DNA) the low-LET dose component is sufficient to fully account for the observed radiation lethality (Fig. 4). If DNA DSB are assumed to be the primary lethal lesion, and if cell death in the 15 min chase group can be attributed to the relatively few DNA DSB produced by the low-LET dose component, it follows that the much more numerous (and probably also more severe) local breaks at the site

of ^{125}I-decay in newly replicated DNA do not contribute to radiation death. Such breaks must therefore be completely repaired. This is contrary to the conventional view that local damage at the site of ^{125}I decay is difficult to repair. Even if we were to grant the possibility that all the local DNA DSB at the decay site could be fully repaired, the existence of such total repair would merely confirm that there is no direct quantitative correlation between DNA DSB and subsequent cell death.

This conclusion is supported by a different line of reasoning. As pointed out above, a low-LET pattern of ^{125}I-induced cell death indicates that the ^{125}I-decays had occurred at a site distant from the primary target for radiation death. From the data shown in Figs. 2 and 4, it is apparent that ^{125}I-decays in newly synthesized DNA (15 min chase group) do not induce high-LET type cell death. It would be difficult to reconcile this finding with the notion that DNA is the sole target for radiation death. Labeled DNA obviously is always located within the high-LET region around the site of ^{125}I-decay and thus invariably sustains high-LET type damage. This suggests that the primary radiation target in mammalian cells is a higher-order structure that is closely associated with DNA in the cell nucleus. This structure may or may not sustain high-LET damage from ^{125}I-decays in the DNA, depending on whether or not the labeled DNA is directly associated with the structure. Viewed from this perspective, our findings in conjunction with similar discrepancies between DNA damage and cell death reported earlier (28,29,31-33), contradict the widely held view that DNA DSB are directly linked to cellular radiation death.

Alternative Target Structures for Cell Death

The suggestion that damage to DNA may not be the sole mechanism for radiation death, although startling, is not novel. Alper (34) has long maintained that two types of damage may contribute to radiation death in mammalian cells, type O damage to membranes and type N damage to DNA. Elkind and coworkers have repeatedly interpreted their data as indicating that DNA may be closely associated with a non-DNA target capable of accumulating sublethal damage (35,36). Cole (37) suggested that toxic products from radiation-induced peroxidation of lipids may induce configurational damage in chromatin and/or supporting structures in the nuclear matrix. Recent findings by Yasui *et al.* (31) support this view and suggest that damage to higher-order chromatin structures may be responsible for radiation death.

The notion that higher-order structures within the cell nucleus may play a decisive role in the genesis of cellular radiation death is in accord with current knowledge on the organization of the genome (38). At least three higher levels of DNA organization (nucleosome, solenoid, DNA loop domain) have been identified and found to interact with the nuclear matrix in a dynamic structural arrangement. Various components of the nuclear matrix appear to be intimately involved in DNA synthesis, RNA transcription, DNA processing and transport, and possibly also DNA repair. Other attachment points of the DNA at the nuclear matrix are believed to be involved in chromosome condensation during mitosis and meiosis. In short, proper functioning of the genome appears to demand a spatial and temporal precision that would be unattainable in the absence of structural order. Given the complexity of genome organization it would not be surprising if damage to this structural order were the ultimate cause of radiation death. In fact, it is conceivable that disruption of the structural hierarchy within the cell nucleus may in itself be sufficient to cause cell death without any accompanying damage to the linear sequence of DNA.

The hypothesis that DNA damage *per se* may not be the sole mechanism for radiation death provides a cohesive and internally consistent interpretation for our results. It explains the finding that the cytocidal effects of ^{125}I increase as the length of the post-labeling chase period is increased (Fig. 2), whereas no such effect is observed with X ray exposures (Fig. 3). Most of the nucleoprotein would be associated with other nuclear structures such as the nuclear matrix throughout the cell cycle and external X irradiation would disrupt this structural arrangement whether or not any particular DNA segment is attached to it. In contrast, ^{125}I incorporated into newly replicated segments of DNA would initially not be directly associated with the target structure. Thus, ^{125}I-decays in newly replicated DNA would not be expected to reach full toxic potential until the labeled DNA segments had established close contact with (or become part of) higher-order structures. At that stage, Auger electrons originating from ^{125}I-decays in the DNA would be able to induce high-LET damage not only in DNA, but also in the DNA-containing superstructure, causing greatly enhanced cell death.

It should be noted that the chase experiments described above could not be duplicated with any external radiation source, high-LET or low-LET, because external radiations would not permit selective irradiation of newly replicated portions of the genome. This demonstrates again the unique features of ^{125}I-decay and its utility for dissecting the molecular mechanisms

of radiation damage. In many ways, the difference between ^{125}I and external radiations is analogous to the difference between smart bombs and conventional bombs. ^{125}I acts like a smart bomb that destroys individual components of the system, with only minor collateral damage to distant sites. Exposure to external radiations is comparable to large-area carpet bombing that indiscriminately damages the system as a whole.

CONCLUSIONS

The data reported here indicate that, depending on the labeling conditions and the duration of the post-labeling chase, ^{125}I incorporated into DNA can act either as a low-LET or high-LET radiation source. If a sufficient time interval (about 5 h) is allowed to elapse between ^{125}I incorporation and decay accumulation, DNA-bound ^{125}I induces high-LET like cytocidal effects regardless of whether decays are randomly distributed over the entire genome (continuous labeling) or restricted to different 2-5% subfractions of the genome (10 min pulse-labeling). However, if pulse-labeled cells are harvested for decay accumulation within 1 h of labeling, ^{125}I-decays in the DNA yield a low-LET dose-survival curve comparable to that obtained with external X ray exposures. This paradox can be explained by postulating that damage to high-level structures within the cell nucleus (*e.g.*, solenoids, DNA loop domains and/or associated nuclear matrix elements) constitutes the primary mechanism for radiation-induced cell death.

REFERENCES

1. K.G. HOFER, W. PRESNKY, and W.L. HUGHES, Death and metastatic distribution of tumor cells in mice monitored with ^{125}I-iododeoxyuridine. *J. Nat. Cancer Inst.* **43**, 763-773 (1969).
2. H.H. ERTL, L.E. FEINENDEGEN, and J. HEINIGER, ^{125}I, a tracer in cell biology: Physical properties and biological aspects. *Phys. Med. Biol.* **15**, 447-456 (1970).
3. K.G. HOFER and W.L. HUGHES, Radiotoxicity of intranuclear tritium, 125-iodine and 131-iodine. *Radiat. Res.* **47**, 94-109 (1971).
4. L.E. FEINENDEGEN, H.H. ERTL, and V.P. BOND, Biological toxicity associated with the Auger effect. In *Biophysical Aspects of Radiation Quality*, pp. 419-430. IAEA, Vienna, 1971.
5. K.G. HOFER, C.R. HARRIS, and J.M. SMITH, Radiotoxicity of intracellular ^{67}Ga, ^{125}I and ^{3}H: Nuclear versus cytoplasmic radiation effects in murine L1210 leukemia. *Int. J. Radiat. Biol.* **28**, 225-241 (1975).

6. A.I. KASSIS and S.J. ADELSTEIN, Radiotoxicity of ^{75}Se and ^{35}S: Theory and application to a cellular model. *Radiat. Res.* **84**, 407-425 (1980).
7. A.I. KASSIS, S.J. ADELSTEIN, C. HAYDOCK, K.S.R. SASTRY, K.D. McELVANY, and M.J. WELCH, Lethality of Auger electrons from the decay of bromine-77 in the DNA of mammalian cells. *Radiat. Res.* **91**, 362-373 (1982).
8. D.E. CHARLTON and J. BOOZ, A Monte Carlo treatment of the decay of ^{125}I. *Radiat. Res.* **87**, 10-23 (1981).
9. K.G. HOFER, G. KEOUGH, and J.M. SMITH, Biological toxicity of Auger emitters: Molecular fragmentation versus electron irradiation. *Cur. Top. Radiat. Res. Q.* **12**, 335-354 (1977).
10. R.E. ZIRKLE and W. BLOOM, Irradiation of parts of individual cells. *Science* **117**, 487-493 (1953).
11. T.R. MUNRO, The relative radiosensitivity of the nucleus and cytoplasm of Chinese hamster fibroblasts. *Radiat. Res.* **42**, 451-470 (1970).
12. R.L. WARTERS, K.G. HOFER, C.R. HARRIS, and J.M. SMITH, Radionuclide toxicity in cultured mammalian cells: Elucidation of the primary site for radiation damage. *Cur. Top. Radiat. Res. Q.* **12**, 389-407 (1977).
13. L.S. YASUI and K.G. HOFER, Role of mitochondrial DNA in cell death induced by ^{125}I decay. *Int. J. Radiat. Biol.* **49**, 601-610 (1986).
14. M.H. SCHNEIDERMAN, K.G. HOFER, and G.S. SCHNEIDERMAN, An in vitro ^{125}IUdR-release assay for measuring the kinetics of cell death. *Int. J. Radiat. Biol.* **59**, 397-408 (1991).
15. M.H. SCHNEIDERMAN, K.G. HOFER, and G.S. SCHNEIDERMAN, Cell cycle progression after selective irradiation of DNA during the cell cycle. *Radiat. Res.* **116**, 283-291 (1988).
16. M.H. SCHNEIDERMAN and K.G. HOFER, The target for radiation-induced division delay. *Radiat. Res.* **84**, 462-476 (1980).
17. M.H. SCHNEIDERMAN, W.C. DEWEY, D.B. LEEPER, and H. NAGASAWA, Use of the mitotic selection procedure for cell cycle analysis. Comparison between the X ray and cyclohexamide G_2 markers. *Exp. Cell Res.* **74**, 430-438 (1972).
18. W.G. KEOUGH and K.G. HOFER, An improved method for synthesis and purification of ^{125}I or ^{131}I labeled carrier-free 5-iodo-2'-deoxyuridine. *J. Lab. Comp. Radiopharm.* **14**, 83-90, (1978).
19. G. PEDRALI-NOY, S. SPADARI, A. MILLER-FAURES, A.O.A. MILLER, J. KRUPPA, and G. KOCH, Synchronization of HeLa cell cultures by inhibition of DNA polymerase alpha with aphidicolin. *Nucl. Acid Res.* **8**, 377-387 (1980).
20. S.L. COMMERFORD, V.P. CRONKITE, and U. REINCKE, The effect of changes in cell geometry associated with freezing on the radiation dose from decay of internal isotopes. *Int. J. Radiat. Biol.* **41**, 99-103 (1982).
21. H.G. PARETZKE, Radiation track structure theory. In *Kinetics of Nonhomogenesis Processes* (G.R. FREEMAN, Ed.), pp. 89-170, Wiley, New York, 1987.
22. D.E. CHARLTON and J.L. HUMM, A method of calculating initial DNA strand breakage following the decay of incorporated ^{125}I. *Int. J. Radiat. Biol.* **53**, 353-365 (1988).
23. E. POMPLUN, A new DNA target model for track structure calculations and its first application to I-125 Auger electrons. *Int. J. Radiat. Biol.* **59**, 625-642 (1991).

24. R.B. PAINTER, The role of DNA damage and repair in cell killing induced by ionizing radiation. In *Radiation Biology in Cancer Research* (R.E. MEYN and H.R. WITHERS, Eds.), pp. 59-68, New York, Raven Press, 1980.
25. I.R. RADFORD, G.S. HODGSON, and J.P. MATTHEWS, Critical DNA target size model of ionizing radiation-induced mammalian cell death. *Int. J. Radiat. Biol.* **54**, 63-79 (1988).
26. R.F. MARTIN and W.A. HASELTINE, Range of radiochemical damage to DNA with decay of iodine-125. *Science* **213**, 896-898 (1981).
27. I.R. RADFORD and G.S. HODGSON, ^{125}I-induced DNA double strand breaks: Use in calibration of the neutral filter elution technique and comparison with X ray induced breaks. *Int. J. Radiat. Biol.* **48**, 555-566 (1985).
28. H.L. LIBER, P.K. LeMOTTE, and J.B. LITTLE, Toxicity and mutagenicity of X rays and [^{125}I]dUrD or [^{3}H]TdR incorporated in the DNA of human lymphoblast cells. *Mutat. Res.* **111**, 387-404 (1983).
29. P.K. LEMOTTE and J.B. LITTLE, DNA damage induced in human diploid cells by decay of incorporated radionuclides. *Cancer Res.* **44**, 1337-1342 (1984).
30. M. LJUNGMAN, The influence of chromatin structure on the frequency of radiation-induced DNA strand breaks: a study using nuclear and nucleoid monolayers. *Radiat. Res.* **126**, 58-64 (1991).
31. L.S. YASUI, A.S. PASCHOA, R.L. WARTERS, and K.G. HOFER, Cytotoxicity of ^{125}I decay produced lesions in chromatin. In *DNA Damage by Auger Emitters* (K.F. BAVERSTOCK and D.E. CHARLTON, Eds.), pp. 181-189, Taylor and Francis, London, 1988.
32. I.R. RADFORD and S. BROADHURST, Aphidicolin synchronization of mouse L cells perturbs the relationship between cell killing and DNA double-strand breakage after X-irradiation. *Int. J. Radiat. Biol.* **53**, 205 -215 (1988).
33. G. ILIAKIS, L. METZGER, R.J. MUSCHEL, and W. GILLIES McKENNA, Induction and repair of DNA double strand breaks in radiation-resistant cells obtained by transformation of primary rat embryo cells with the oncogenes H-ras and v-myc. *Cancer Res.* **50**, 6575-6579 (1990).
34. T. ALPER, *Cellular Radiobiology*, Cambridge University Press, Cambridge, 1979.
35. E. BEN-HUR and M.M. ELKIND, Thermally enhanced radioresponse of cultured Chinese hamster cells: Damage and repair of single-strand DNA and a DNA complex. *Radiat. Res.* **59**, 484-495 (1974).
36. M.M. ELKIND and J.I. REDPATH, Molecular and cellular biology of radiation lethality. In *Cancer, A Comprehensive Treatise*, Vol. 6 (F. F. BECKER, Ed.), pp. 51-99, Plenum Publishing Company, New York, 1977.
37. A. COLE, Radiation effects on DNA and membranes. In *Proc. 7th Int. Cong. Radiat. Res.* (J.J. BROERSE, G.W. BARENDSEN, H.B. KAL, and A.J. VAN DER VOGEL, Eds.), pp. 225-230, Martinus Nijhoff, Amsterdam, 1983.
38. W.G. NELSON, K.J. PIENTA, E.R. BARRACK, and D.S. COFFEY, The role of the nuclear matrix in the organization and function of DNA. *Ann. Rev. Biophys. Chem.* **15**, 457-475 (1986).

DISCUSSION

Nagasawa, H. N. 1) What concentration of ^{125}IUdR did you apply for the 10 min pulse label? 2) What percent of cells did you recover after the aphidicolin block? 3) Did all labeled cells moving into the next cell cycle have a normal chromosome component? Were there any ploidy changes and chromosomal aberrations in the nucleus for different labeling times?

Hofer, K. G. 1) For 10 min pulse-labeling we used 10-28 kBq/ml of ^{125}IUdR, giving us an exposure rate of about 0.5-1.0 ^{125}I decays/cell/h at the time of cell harvest and freezing. 2) We used an aphidicolin dose of 5 μg/ml administered to G_1 cells for 7 hours. This treatment regimen did not reduce the survival fraction of cells as compared to control cells that had not been treated with aphidicolin. 3) We have not yet done any studies on chromosome damage or ploidy changes after aphidicolin treatment. As far as the labeling pattern is concerned, we had exceedingly good cell synchrony and our labeling index for pulse-labeled cells was close to one.

DeSombre, E. R. If different organizational forms are involved would you not expect to see different morphological effects (*i.e.* chromosomal damage)?

Hofer, K. G. This is one of the long-range goals of our work. We have shown here that one type of genome damage - DNA DSB - is apparently not quantitatively linked to radiation death. It is conceivable that chromosome breaks will turn out to be directly proportional to cell death. If so, this would be a strong argument that chromosome breaks, rather than DNA DSB, are the ultimate cause of radiation death.

Rao, D. V. Dr. Hofer, I would like your opinion about the nature of the radiosensitive targets. Dudley Goodhead several years ago suggested that the size of the radiosensitive target is about 5 nm in radius based on his soft X ray work. Several years ago our group postulated that these targets may be nucleosome units. Do you think that nucleosomes might be the targets based on your work?

Hofer, K. G. I agree with you that the sensitive target for radiation death is not DNA *per se*, but a higher-order DNA-protein structure. The nucleosome is a potential candidate, but the kinetics of nucleosome formation argues against this possibility. Nucleosome formation is complete within minutes after DNA replication, whereas in our experiments it takes several hours before nearly replicated DNA becomes fully associated with the higher-order target structure. For this reason I believe that the sensitive structure must be a more central structure such as, for example, the DNA-

protein subunit that forms the backbone of the chromosomes. However, this is still speculation and we cannot at this stage exclude the nucleosome or any other higher-order structure closely associated with DNA.